International Journal of Innovative Engineering Applications

Journal homepage: https://dergipark.org.tr/ijiea

PVA/WHEY PROTEIN NANOFIBER-COATED PP MELT BLOWN INTEGRATED WITH PICKERING EMULSION OF CITRAL STABILIZED FOR POTENTIAL MEDICAL APPLICATIONS

***Fatma Nur Parın*[*1], *Ayşenur Yeşilyurt*[1], *Uğur Parın*[2]**

[1]*Department of Polymer Materials Engineering, Faculty of Engineering and Natural Sciences, Bursa Technical University, Bursa, Turkey*
[2]*Department of Chemical Engineering, Faculty of Engineering and Natural Sciences, Bursa Technical University, Bursa, Turkey*
[3]*Department of Microbiology, Faculty of Veterinary Medicine, Aydın Adnan Menderes University, Aydın, Turkey*

Abstract

Original scientific paper

As an antibacterial agent with pleasant fragrance, citral (CIT) indicates hydrophobic character, and therefore has low water solubility. In this study, Pickering emulsions were formed and polyvinyl alcohol (PVA)/whey protein hydrophilic nanofibers were coated on PP melt blown non-woven surfaces by electrospinning method. In this context, hydrophobic citral essential oil is stabilized with β-cyclodextrin (β-CD) in the electrospinning process. PVA and whey protein polymer blend were used as nanofiber matrices. The morphological, physical, and thermal properties of the β-CD/citral complexes were investigated in PVA/whey protein nanofiber-coated PP non-wovens at various β-CD levels (1:2, 1:4 and 1:6). Furthermore, zone inhibition procedure was performed to evaluate antibacterial activity of the samples against Gram (+) (*Staphylococcus aureus* ATCC® 25923) and Gram (-) (*Escherichia coli* ATCC® 25922, and *Pseudomonas aeruginosa* ATCC® 27853) bacteria. The morphology of fibers showed that all obtained nanofiber-coated PP surfaces were in the range with 216 - 330 nm average fiber diameter. Fourier Transform Infrared (FT-IR) and thermal gravimetric analysis (TGA) thermograms revealed that citrals were successfully integrated into the bio-based nanofibers. As the amount of citral increased (i.e., the β-CD/citral increased), the thermal resistance of bio-based nanofiber coated PP surfaces increased. Antibacterial activity indicated the citral-loaded nanofiber-coated PP surfaces were most effective against *Escherichia coli,* while none of the samples have antibacterial activity against *Pseudomonas aeruginosa*. Overall, the results displayed that the fabricated PVA/whey protein nanofiber-coated PP samples integrated with Pickering emulsion of citral stabilized have promising wound dressing applications.

Keywords: *Antibacterial property, Pickering emulsion, PP melt blown, PVA/whey protein nanofiber, β-CD/citral comple.*

POTANSİYEL MEDİKAL UYGULAMALAR İÇİN PVA/WHEY PROTEİN NANOLİF KAPLI PP ERİYİK ÜFLEMELİ DOKUSUZ YÜZEYLERE ENTEGRE EDİLMİŞ SİTRAL STABİLİZE PİCKERİNG EMÜLSİYONLAR

Özet

Orijinal bilimsel makale

Hoş kokulu bir antibakteriyel madde olarak sitral (SIT) hidrofobik karakter sergiler ve bu sebeple suda çözünürlüğü düşüktür. Bu çalışmada Pickering emülsiyonları oluşturulmuş ve elektroçekim yöntemi ile polipropilen (PP) eriyik üflemeli dokusuz yüzeylere polivinil alkol (PVA)/whey proteini hidrofilik nanofiberler kaplanmıştır. Bu bağlamda, elektroçekim yönteminde hidrofobik sitral uçucu yağı β-siklodekstrin (β-CD) ile stabilize edilmiştir. Nanofiber matris olarak PVA ve whey proteini polimer karışımı kullanılmıştır. β-CD/sitral komplekslerinin morfolojik, fiziksel ve termal özellikleri PVA/whey proteini nanofiber kaplı PP dokusuz dokumalarda çeşitli β-CD seviyelerinde (1: 2, 1: 4 ve 1:6) araştırılmıştır. Ayrıca, numunelerin Gram (+) (*Staphylococcus aureus* ATCC ® 25923) ve Gram (-) (*Escherichia coli* ATCC ® 25922 ve *Pseudomonas aeruginosa* ATCC ® 27853) bakterilerine karşı antibakteriyel aktivitesini değerlendirmek için zon inhibisyon prosedürü uygulanmıştır. Liflerin morfolojisi, elde edilen tüm nanofiber kaplı PP yüzeylerin 216 - 330 nm ortalama lif çapı aralığında olduğunu göstermiştir. Fourier Dönüşümü Kızılötesi (FT-IR) spektroskopisi ve termal gravimetrik analiz (TGA) termogramları, sitralin biyo bazlı nanofiberlere başarıyla entegre edildiğini ortaya koymuştur. Sitral miktarı arttıkça (yani β-CD/sitral arttıkça), biyobazlı nanofiber kaplı PP yüzeylerin ısıl direnci artmıştır. Antibakteriyel aktivite, sitral yüklü nanofiber kaplı PP yüzeylerinin *Escherichia coli* bakterisine karşı en etkili olduğunu gösterirken, örneklerin hiçbirinin *Pseudomonas aeruginosa* bakterisine karşı antibakteriyel aktivitesi olmadığını göstermiştir. Genel olarak, sonuçlar, sitral stabilize Pickering emülsiyonu ile entegre edilmiş PVA/whey proteini nanofiber kaplı PP örneklerinin umut verici yara pansuman uygulamalarına sahip olduğunu göstermiştir.

Anahtar Kelimeler: *Antibakteriyel özellik, Pickering emülsiyon, PP melt blown, PVA/whey protein nanolif, β-CD/sitral kompleks.*

[*]Corresponding author.
E-mail address: nur.parin@btu.edu.tr (F. N. Parın)
Received 21 November 2022; Received in revised form 16 November 2023; Accepted 26 April 2024
 Doi: https://doi.org/10.46460/ijiea.1206901

1 Introduction

Essential oils (EOs) have been the focus of considerable investigation as natural products, and they play a crucial role in food and human health [1]. Due to their bioactivity to prevent the development of microorganisms such as bacteria, yeasts, and fungus, the components of essential oils are a promising substitute to chemical preservatives. Citral (3,7-dimethyl-2,6-octadienal) is a combination of two monoterpene aldehydes found naturally in plants, herbs, and citrus fruits: geranial (trans-citral, citral A) and neral (cis-citral, citral B) [2-4]. It has been reported to have anti-inflammatory and anti-corrosive characteristics in a variety of experimental and clinical studies, and there is substantial proof that it functions as a fungicidal and bactericidal agent [5,6]. However, one of the key challenges in the application of citral essential oils and their principal components is the requirement for greater amounts than those utilized in vitro. One alternative option is to combine oils and/or components to reduce the amount required [7]. Other factors restricting the use of citral in many applications are its low water solubility and sensitivity to environmental influences such as thermal and oxidation. In this regard, it has been found that making emulsions of citral oil increases the availability and shelf life of different forms such as nanofibers, microcapsules, films, as well as its antibacterial activity. According to Lu et al. (2018) essential oil nanoemulsions containing citral had a substantial effect on Gram (+) bacteria, the bacteria with the highest zone of inhibition test [3]. Mokarizadeh et al. (2017) have investigated the antimicrobial activity of citral loaded nanocarriers [8]. They assigned activity of citral with good values against many microorganisms. In addition, there are quite a lot of studies in the literature on the production of electrospun fibers after emulsifying essential oils in water-based polymer solutions.

Nanofibers, one of several polymeric forms, are complex fibrous structures with sizes ranging from micrometers to nanometers [9-14]. Because of their high porosity, wide specific surface area, and relatively small size, nanofibers have become a promising choice for medical applications over the last few decades.

Pickering emulsions are a unique approach of stabilizing emulsions, i.e., oil/water mixtures, that utilize solid particles instead of surfactants [15]. In this approach, in this approach, by using inorganic particles such as modified clay, silica, the emulsion is stabilized and a barrier is formed that prevents the formation of cohesiveness. Thus, stable emulsion solutions are obtained.

β-cyclodextrin is a kind of carbohydrate and it has hollow conical shape with hydrophilic outer part and hydrophobic inner part which makes it an excellent Pickering emulsifier [16]. Therefore, stable emulsions have better evaporation resistance to essential oils than surfactant-stabilized systems, giving better antibacterial performance thanks to the β-cyclodextrin.

The current study concerned with fabrication of PVA/whey protein/citral nanofiber-coated PP melt blown surfaces by using 3 various ratio of β-CD/citral complexes (1:2, 1:4 and 1:6) via electrospinning. For this aim, due to the low solubility of citral in water, o/w Pickering emulsion solutions were obtained by adding the antibacterial citral agent to β-CD-stabilized biobased PVA hydrophilic solutions. Afterward, the bio-based o/w polymer solutions were coated on the PP melt blown surfaces by electrospinning. The findings showed that nanofiber solutions up to certain β-CD/citral (1:4) ratio show good fiber morphology, while the nanofiber solution with the highest β-CD/citral (1:6) ratio show the highest antibacterial activity against *Escherichia coli* (*E.coli).* Finally, it is suggested that PVA/whey protein/citral nanofiber-coated PP melt blown surfaces can be good candidates for medical usages especially wound dressing applications.

2 Materials and Method

2.1 Materials

PP meltblown (MB) non-woven fabrics were kindly donated by Mogul Textile Company (Gaziantep, Turkey) were used. The polyvinyl alcohol (PVA) (purity 87.8%, Mw~30.000 g/mol) was purchased from Zag Industrial Chemical Company (Turkey). Whey protein powders were used which purchased from Naturebyme (İstanbul, Turkey). β-cyclodextrin (β-CD) cyclodextrin (β-CD) (Cavamax W7 HP Pharma) was donated by Wacker Chemie (Germany). Citral ($C_{10}H_{16}O$) (technical grade) was kindly donated by Elso Kimya Chemical Company (Turkey). All of the chemicals were used without being purified in the experiments.

2.2 Fabrication of Citral-Loaded Hybride Non-Woven Surfaces

PVA powders dissolved in distilled water to obtain a 10% (w/v) PVA solution by stirring at 90 °C. Whey protein powders were also dissolved in water to obtain 20% (w/v) whey protein solutions. Then, these two polymer solutions were mixed to make blend solutions (7/3, v/v). β-cyclodextrin /citral complexes were added to the polymer mixtures as ratio of 1:2, 1:4 and 1:6 (w/v) and then high-speed mixing was performed. The nanofibers were successfully fabricated onto PP meltblown surfaces via electrospinning (Nanospinner24, INOVENSO). The electrospinning process parameters were given in Table 1. The neat PVA/whey protein nanofiber coated-melt blown hybrid surfaces used as a control sample. All samples was kept in the desicator. The samples were named PPWPC1, PPWPC2, and PPWPC3, where C1, C2, and C3, respectively stand for the changing β-CD/citral ratios (1:2, 1:4, and 1:6). The neat sample was named PPWPC0.

Table 1. The electrospinning process parameters.

	Voltage (kV)	Distance (mm)	Flow rate (mL/h)	Collector rate (rpm)	β-CD/citral (w/v)
PPWPC0	28	89	0.75	250	-
PPWPC1	28	89	0.75	250	1:2
PPWPC2	28	89	0.75	250	1:4
PPWPC3	28	89	0.75	250	1:6

**The temperature and humidity conditions are approximately 26°C and 50 %, respectively.

2.3 Characterization

The nanofibers' microstructural properties was evaluated using a Scanning Electron Microscope (SEM). All samples were gold-coated prior to analysis. Image J (version 1.520 software) was performed to measured fiber diameter for each sample.

Thermogravimetric analysis (TGA) was performed in a nitrogen atmosphere $(N_2)_{(g)}$ with a heating rate of 10°C min^{-1} over a temperature range of 30 – 600 °C, followed by an oxygen atmosphere $(O_2)_{(g)}$ with the same heating rate.

The chemical structures of the non-woven surfaces were confirmed using Fourier transform infrared (FT-IR) spectroscopy. The data were obtained using a ThermoNicolet iS50 FT-IR (USA) spectrometer with an ATR adaptor (Smart Orbit Diamond, USA) in the wavelength range 4000 - 500 cm^{-1}, with 16 scans at 4 cm^{-1} resolution.

2.4 Antibacterial Activity

The antibacterial sensitivities of hybride non-wovens were determined by the standard strains of *Escherichia coli* ATCC® 25922, *Staphylococcus aureus* ATCC® 25923 and *Pseudomonas aeruginosa* ATCC® 27853. The lyophilized bacterial strains were grown on Trypton Soy Agar (Merck Millipore™ 105458). The culture media were incubated for 24 hours at 37°C under aerobic environment. Bacterial colonies were suspended in saline isotonic solution and adjusted to 0.5 McFarland (1 × 108 CFU/mL) turbidity standard.

The disk diffusion technique was used to assess antimicrobial effectiveness qualitatively. Mueller Hinton Agar (Merck MilliporeTM 103872) was inoculated with 100 µL of bacterial suspensions. The polymer ingredients were placed on the agar plate's surface. The plates were incubated in an aerobic atmosphere for 24 hours. At the end of the incubation time, the zone diameter of the inhibition region around the material injected for each non-woven based-polymer was measured using a calliper.

3 Results and Discussion

3.1 Morphological Analysis

SEM analysis was carried out to describe the interior morphology of all nanofiber coatings and the resultant nicrographs are shown in Figure 1. The neat samples (PVA/whey protein) are continuous, with average fiber diameters of 330.5 ± 87 nm. Moreover, uniform and beadless fiber morphology was seen which coincides with the other PVA/whey protein nanofiber morphology in the literature [17]. Fiber diameter distribution of PWPC1 is more homogeneous than the PVA/whey protein/citral fiber coatings (PWPC2 and PWPC3). However, increasing the amount of citral damaged the fiber morphology, resulting in the formation of beaded structures. This is due to the decreasing of spinning solution viscosity. The viscosity of the spinning solutions was a significant parameter influencing the fiber diameter. Kim et al. (2016) also showed that the viscosity of the spinning solution may modify the diameter of PVA-based nanofibers, demonstrating that the viscosity of the solution has a relationship between its concentration and nanofiber diameter [18]. A study on characterization of D-limonene loaded-PVA/psyllium husk showed that the more essential oil there is in the spinning solution, the thinner fibers can be obtained [19]. Furthermore, the existence of citral in the fiber indicated that it can be blended effectively with the polymer matrix thanks to the β-CD (Figure 1B1). When the cross-sectional SEM micrographs of the fibers were examined, it was determined that the best coating was in the PP sample, as well (Supplementary S1).

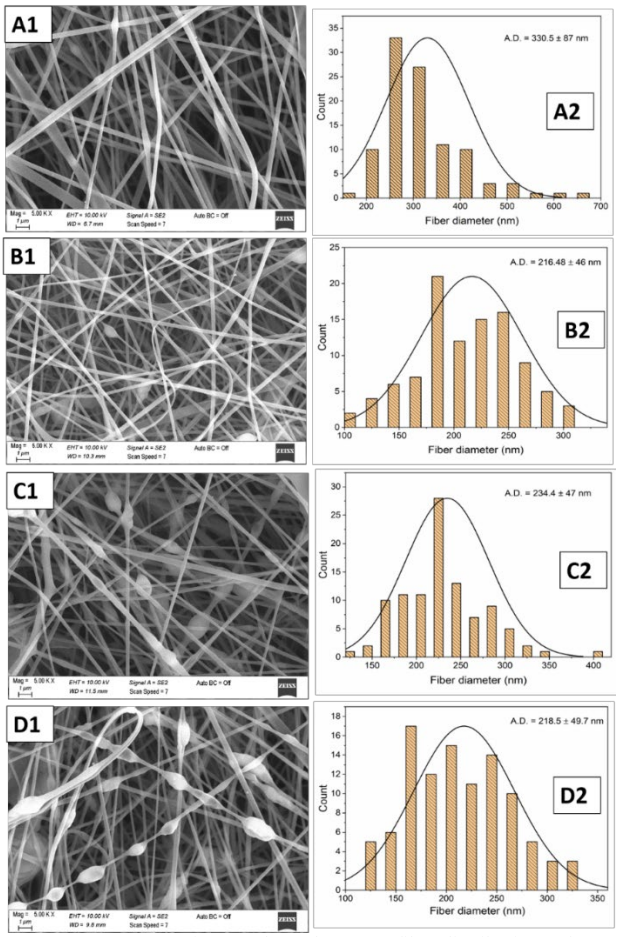

Figure 1. SEM micrographs and average fiber distributions of (A1-A2) neat PVA/whey protein nanofibers (PPWPC0), (B1-B2) PPWPC1 and (C1-C2) PPWPC2, and (D1-D2) PPWPC3.

3.2 FT-IR Spectroscopy

The chemical groups of the neat hybride non-woven and also β-CD/citral loaded non-wovens were investigated by FT-IR (Figure 2). PP melt blown non-woven surfaces' FT-IR spectra showed typical asymmetric and symmetric stretching peaks at 2948 cm^{-1} and 2916 cm^{-1} (-CH) and 2836 cm^{-1}, respectively. The other peaks appear at 1455 cm^{-1}, 1376 cm^{-1}, and 840 cm^{-1} belong to ($-CH_2$) bending [10].

The characteristic absorption bands of PVA are as follows: 3299 cm^{-1} (-OH stretching), 2955 cm^{-1} and 2861 cm^{-1} asymmetric and symmetric (-CH stretching), 1418 cm^{-1} (-OH or -CH bending), 1087 cm^{-1} (C-C stretching and -OH bending), and 840 cm^{-1} (CH_2 rocking) [20,21]. Moreover, based on the literature the FT-IR bands of whey protein appears at ranging from 3100 to 3500 cm^{-1} on protein strings associated with -NH stretching and free -OH group, respectively. The peaks from 2850 cm^{-1} to 2980 cm^{-1} are linked with a C-H stretching, the band between 1600 - 1700 cm^{-1} are related with amide-I (C=O stretching and C-N stretching), the band formed in 1400 to 1550 cm^{-1} related to amide-II (-NH bending), the peaks at 1200 - 1350 cm^{-1} are related to amide-III (-CN stretching and -NH in plane bending vibration) [22-24]. The presence of these bands indicated that whey protein had been absorbed into the PVA blended nanofibers, as did whey protein's triple helix structure. In this context, PPWPC0 sample has typical absorption peaks at 3283 cm^{-1} which is related to PVA and whey protein (-OH stretching and -NH stretching), at 2917 cm^{-1} is -CH stretching, the peaks at 1733 cm^{-1} and 1644 cm^{-1} attributed with a -C=O stretching vibration band from carbonyl functional groups remaining after PVA synthesis from polyvinyl acetate hydrolysis or oxidation during preparation and amide-I, respectively. Amide-II is from whey protein and (-OH) bending from PVA are observed in 1537 cm^{-1} and 1424 cm^{-1}, respectively. The peaks at 1374 cm^{-1}, 1324 cm^{-1}, 1243 cm^{-1} are belongs to amide-III (-CN stretching and -NH bending) and the peaks appears from PVA 1080 cm^{-1} and 1080 cm^{-1} (C-C stretching and -OH bending), 840 cm^{-1} (CH_2 rocking), respectively. The peak value decrease in the peaks of 1080 cm^{-1} and 1030 cm^{-1} assigned with C-C stretching and -OH bending, is also indicated in the PPWPC1, PPWPC2 and PPWPC3 nanofibers by the addition of citral. The FT-IR spectra peaks of citral between 2915 cm^{-1} and 2856 cm^{-1} were assigned to CH_3 and CH_2 stretching vibrations, respectively, as shown in Figure 3. The -C=O stretching vibration peak was at 1671 cm^{-1}, the C=C vibration peak was at 1441 cm^{-1}, and the CH_3 bending vibration absorption peak was at about 1376 cm^{-1} [25,26]. The characteristic peaks of citral overlaid with PVA/whey protein matrix, the matrix spectrum covered the presence of citral. This finding is parallel with the literature. In a study performed on the composite hydrogels, the characteristic peaks of citral are hidden in the polymer matrix [27]. Further, it is assumed that a small amount of citral use also causes this condition. In another study, it was reported that a new peak was formed by adding citral to hydrogels consisting of chitosan and carboxymethyl cellulose [28].

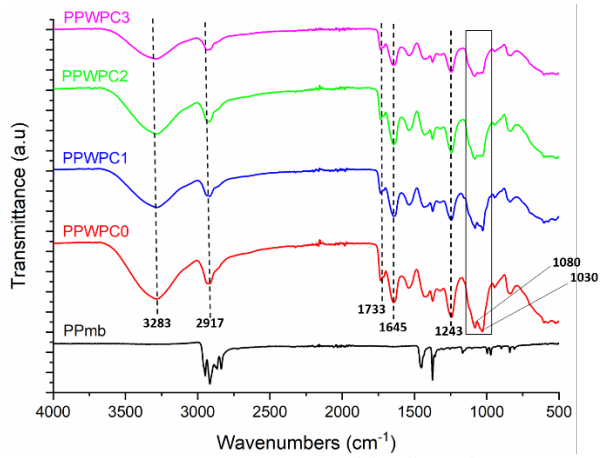

Figure 2. FT-IR spectrum of the all samples.

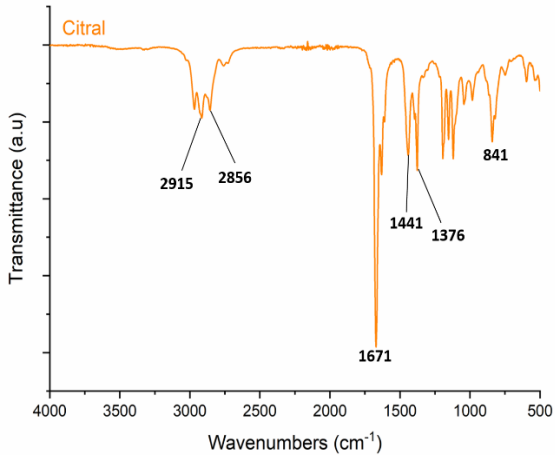

Figure 3. FT-IR spectrum of the citral.

3.3 Thermal Properties

Figure 4 indicates the thermal characteristic of the hybrid fibers. The weight loss of all samples has a slight initial weight loss between 30-100°C due to vaporization of free water. Single-step degradation has been observed for PP melt blown NWs at and 350-470°C (except for moisture loss). The TGA curve of neat PVA/whey protein nanofiber-coated PP non-woven (PPWPC0) and all citral-loaded PVA/whey protein-coated PP non-wovens (PPWPC1, PPWPC2, PPWPC3) samples have the same degradation profile and show 3-step breakdown (except for moisture loss). The initial degradation of neat sample PPWPC0 occurred between 250°C and 400°C, which may be related to both PVA and whey protein degradation. As previously reported, the side chain breakage of PVA started at 200 °C and for whey protein degradation temperature at approximately 270°C, as well [20]. The second degradation step was found between 400 - 500°C. This is due to PVA's backbone breakdown, chain scission of PVA molecules dominated, and also the degradation of side groups that are separated from the whey protein's backbone [21]. After the last step (600 - 625°C) was the of the pyrolysis product produced throughout the analysis in the N2(g) environment. Interestingly, the degradation profiles of the neat sample (PPWPC0) and sample with max β-CD/citral ratio (PPWPC3) are very similar to each other. However, in the second stage, PPWP0 sample has more weight-loss than PPWP3 sample one. With the addition of citral essential oil to the structure, the heat

resistance reduces. It is predicted there is a strong interaction between the polymer matrix (PVA/whey protein) and β-CD/citral complex. It is known that essential oils are sensitive to heat and oxidation, and an increase in the amount of essential oil reduces the thermal resistance of the material in many studies [29].

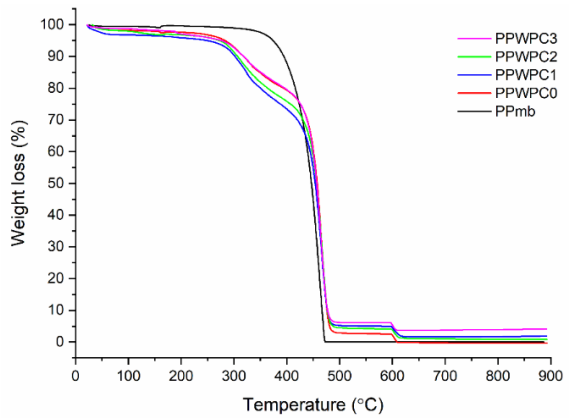

Figure 4. TGA thermograms of all samples.

3.4 Antibacterial Efficiency

The disk diffusion procedure was performed to investigate the antibacterial activity of neat (PPWPC0) and citral-loaded (PPWPC1, PPWPC2, and PPWPC3) samples against three species of bacteria (*E. coli, S. aureus,* and *P. aeruginosa*) (Table 2 and Figure 5).

Bacterial infections seem to be a serious healthcare concern as a result of the proliferation and distribution of multi-drug bacterial resistance, which has attracted the attention of researchers in developing novel antimicrobial therapies [30]. Citral has been shown to be a bacteriostatic agent against *Staphylococcus aureus* [31], *Listeria* [32], and *Escherichia coli* [33], although the antibacterial mechanism has not been investigated further [34]. Citral's antimicrobial activity can damage cell walls of bacteria [3]. A study about the antibacterial mechanism of citral was performed by Tao et al. (2014) [35]. In this study, it is appointed that citral with *Penicillium italicum* provides for a decrease in lipid content in the bacteria, which inhibits membrane stability and enhances permeability of water-soluble compounds.

Despite its effectiveness against harmful microorganisms in many applications such as food,

pharmaceutical, medical, and cosmetic, citral still encounters significant obstacles in terms of use and application. In this regard, fabrication of citral loaded-PVA/whey protein nanofiber-coated PP non-wovens good approach for medical uses. As per Fig. 5, control sample (PWPC0) indicated no zone of inhibition for all bacteria. PPWPC3 sample indicates antibacterial activity against all type of bacteria due to the max β-CD/citral ratio (1:6). Further, all citral-containing samples (PPWPC1, PPWPC2, and PPWPC3) displayed antibacterial activity against *E. coli* bacteria. It is reported Gram (-) bacteria are often more resistant to plant extracts, oils, and their components than Gram (+) bacteria (*S. aureus*), owing to their more complex cell walls [36]. However, in this study samples with citral showed higher antibacterial efficiency against Gram (+) bacteria. Many studies suggest that some biological agents are more effective against Gram-positive bacteria [37,38]. Ma et al. (2020) reported that the synthesized citral-loaded chitosan/carboxymethyl cellulose hydrogels has good antibacterial effect against *E. coli and S. aureus*. [28]. As the β-CD/citral rate increased, the antibacterial activity of the samples increased, in this study. PWPC3 samples have the best antibacterial efficiencies against *Escherichia coli* with 14 mm and zone inhibition.

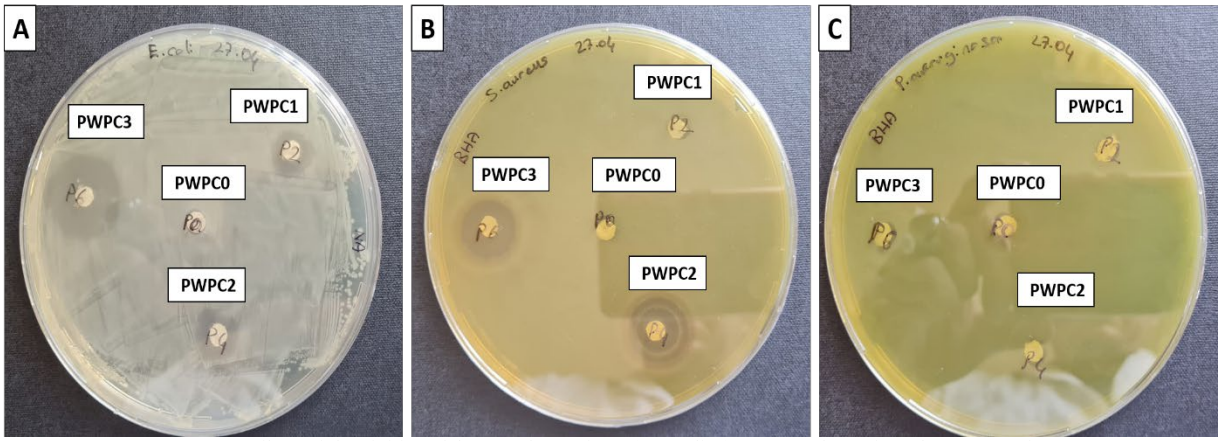

Figure 5. Antibacterial activities of the samples against A) E. coli B) S. aureus bacteria and C) P. aeruginosa

Table 2. Zone inhibition values of the hybride surfaces.

Sample ID	Inhibition Zone (mm)		
	Escherichia coli	*Staphylococcus aureus*	*Pseudomonas aeruginosa*
PPmb	-	-	-
PPWPC0	-	-	-
PPWPC1	8	-	-
PPWPC2	10	10	-
PPWPC3	14	12	-

4 Conclusion

In this study, PP melt blown non-woven surfaces successfully coated with PVA/whey protein/citral nanofibers via electrospinning. Citral was stabilized with β-CD, as a Pickering emulsifier. Therefore, Pickering emulsion solutions were formed to obtain bio-based nanofiber coatings in the electrospinning process. In general, the morphological results of the nanofiber coatings showed that the diameter of the fibers decreases due to the fact that the citral concentration reduces the viscosity of the solution. In addition, it was observed that the fiber morphology of the sample (PPWPC3) with the highest β-CD/citral ratio was disrupted. Nevertheless, it was concluded that the increase in concentration with the results of TGA provides resistance to the degradation of the material due to the interaction between matrix and β-CD/citral complex in the Pickering emulsions. According to FT-IR analysis, the obvious interaction between PVA/whey protein polymer matrices and β-CD/citral complexes has not been detected. The slight changes were appointed in the ranges of 1000 - 1200 cm^{-1} band based on the increase of β-CD/citral complexes. The resulting materials have good antibacterial efficiencies between 8 – 14 mm against *E.coli.* Therefore, these new nanofiber-coated PP melt blowns developed with antibacterial activity might be used to bacterial infections. Nonetheless, more research on the materials' in vitro and in vivo cytotoxicity and wound scratch testing will be required. In summary, our findings provide insight on the role of good antibacterial efficiency as well as production process of new material for medical applications.

Declaration

The authors declare that the ethics committee approval is not required for this study.

References

[1] Zhang, Y., Wei, J., Chen, H., Song, Z., Guo, H., Yuan, Y., & Yue, T. (2020). Antibacterial activity of essential oils against Stenotrophomonas maltophilia and the effect of citral on cell membrane. *LWT, 117:108667.*

[2] Souza, V. V. M. A., Almeida, J. M., Barbosa, L. N., & Silva, N. C. C. (2022). Citral, carvacrol, eugenol and thymol: antimicrobial activity and its application in food. *Journal of Essential Oil Research*, 1-14.

[3] Saddiq, A. A., & Khayyat, S. A. (2010). Chemical and antimicrobial studies of monoterpene: Citral. *Pesticide Biochemistry and Physiology*, 98(1), 89-93.

[4] Lu, W. C., Huang, D. W., Wang, C. C., Yeh, C. H., Tsai, J. C., Huang, Y. T., & Li, P. H. (2018). Preparation, characterization, and antimicrobial activity of nanoemulsions incorporating citral essential oil. J*ournal of food and drug analysis,* 26(1), 82-89.

[5] Shi, C., Song, K., Zhang, X., Sun, Y., Sui, Y., Chen, Y., Xia, X. (2016). Antimicrobial activity and possible mechanism of action of citral against *Cronobacter sakazakii. Plos one,* 11(7):e0159006.

[6] Silva, C. D. B. D., Guterres, S. S., Weisheimer, V., & Schapoval, E. E. (2008). Antifungal activity of the lemongrass oil and citral against Candida spp. *Brazilian Journal of Infectious Diseases,* 12(1), 63-66.

[7] Chao, S. C., Young, D. G., & Oberg, C. J. (2000). Screening for inhibitory activity of essential oils on selected bacteria, fungi and viruses. *Journal of essential oil research,* 12(5), 639-649.

[8] Mokarizadeh, M., Kafil, H. S., Ghanbarzadeh, S., Alizadeh, A., & Hamishehkar, H. (2017). Improvement of citral antimicrobial activity by incorporation into nanostructured lipid carriers: a potential application in food stuffs as a natural preservative. *Research in Pharmaceutical Sciences,* 12(5), 409.

[9] Parin, F. N., Terzioğlu, P., Sicak, Y., Yildirim, K., & Öztürk, M. (2021). Pine honey–loaded electrospun poly (vinyl alcohol)/gelatin nanofibers with antioxidant properties. *The Journal of The Textile Institute,* 112(4), 628-635.

[10] Parın, F. N., & Yıldırım, K. (2021). Preparation and characterisation of vitamin-loaded electrospun nanofibres as promising transdermal patches. *Fibres & Textiles in Eastern Europe.*

[11] Parın, F. N., Aydemir, Ç. İ., Taner, G., & Yıldırım, K. (2021). Co-electrospun-electrosprayed PVA/folic acid nanofibers for transdermal drug delivery: Preparation, characterization, and in vitro cytocompatibility. *Journal of Industrial Textiles,* 1528083721997185.

[12] Parın, F. N., & Parın, U. (2022). Spirulina Biomass-Loaded Thermoplastic Polyurethane/Polycaprolacton (TPU/PCL) Nanofibrous Mats: Fabrication, Characterization, and Antibacterial Activity as Potential Wound Healing. *ChemistrySelect,* 7(8):e202104148.

[13] Parin, F. N., & Terzioğlu, P. (2022). Electrospun Porous Biobased Polymer Mats for Biomedical Applications, In Advanced Functional Porous Materials. *Springer, Cham.,* 539-586.

[14] Çobanoğlu, B., Parin, F. N., & Yildirim, K. (2021). Production and characterization of n-halamine based polyvinyl chloride (pvc) nanowebs. *Textile and Apparel*, 31(3), 147-155.

[15] Hu, J. W., Yen, M. W., Wang, A. J., & Chu, I. M. (2018). Effect of oil structure on cyclodextrin-based Pickering emulsions for bupivacaine topical application. *Colloids and Surfaces B: Biointerfaces*, 161, 51-58.

[16] Li, C., Luo, X., Li, L., Cai, Y., Kang, X., & Li, P. (2022). Carboxymethyl chitosan-based electrospun nanofibers with high citral-loading for potential anti-infection wound dressings. *International Journal of Biological Macromolecules*, 209, 344-355.

[17] Tatlisu, N. B., Yilmaz, M. T., & Arici, M. (2019). Fabrication and characterization of thymol-loaded nanofiber mats as a novel antimould surface material for coating cheese surface. *Food Packaging and Shelf Life,* 21:100347.

[18] Kim, J. H., Lee, H., Jatoi, A. W., Im, S. S., Lee, J. S., & Kim, I. S. (2016). Juniperus chinensis extracts loaded PVA nanofiber: *Enhanced antibacterial activity. Materials* Letters, 181, 367–370.

[19] Parın, F. N., Ullah, A., Yeşilyurt, A., Parın, U., Haider, M. K., & Kharaghani, D. (2022). Development of PVA–psyllium husk meshes via emulsion electrospinning: Preparation, characterization, and antibacterial activity. *Polymers,* 14(7), 1490.

[20] Iqbal, B., Muhammad, N., Rahim, A., Iqbal, F., Sharif, F., Safi, S. Z., ... & Rehman, I. U. (2019). Development of collagen/PVA composites patches for osteochondral defects using a green processing of ionic liquid. *International Journal of Polymeric Materials and Polymeric Biomaterials,* 68(10), 590-596.

[21] El Moujahed, S., Errachidi, F., Abou Oualid, H., Botezatu-Dediu, A. V., Chahdi, F. O., Rodi, Y. K., & Dinica, R. M. (2022). Extraction of insoluble fibrous collagen for characterization and crosslinking with phenolic compounds from pomegranate byproducts for leather tanning applications. *RSC advances,* 12(7), 4175-4186.

[22] Agudelo-Cuartas, C., Granda-Restrepo, D., Sobral, P. J., & Castro, W. (2021). Determination of mechanical properties of whey protein films during accelerated aging: application of FTIR profiles and chemometric tools. *Journal of Food Process Engineering,* 44(5):e13477.

[23] Agudelo-Cuartas, C., Granda-Restrepo, D., Sobral, P. J., Hernandez, H., & Castro, W. (2020). Characterization of whey protein-based films incorporated with natamycin and nanoemulsion of α-tocopherol. *Heliyon,* 6(4):e03809.

[24] Ghadetaj, A., Almasi, H., & Mehryar, L. (2018). Development and characterization of whey protein isolate active films containing nanoemulsions of Grammosciadium ptrocarpum Bioss. essential oil. *Food packaging and shelf life,* 16, 31-40.

[25] Tian, H., Lu, Z., Li, D., & Hu, J. (2018). Preparation and characterization of citral-loaded solid lipid nanoparticles. *Food Chemistry*, *248*, 78-85.

[26] Zhou, W., Lin, J., Wu, R., Lin, W., Ge, F., & Huang, H. (2005). Direct synthesis of lemonile from litsea cubeba oil. *Fine Chem*, *22*, 515-517.

[27] Peng, R., Zhang, J., Du, C., Li, Q., Hu, A., Liu, C., ... & Yin, W. (2021). Investigation of the Release Mechanism and Mould Resistance of Citral-Loaded Bamboo Strips. *Polymers*, *13*(19), 3314.

[28] Ma, H., Zhao, Y., Lu, Z., Xing, R., Yao, X., Jin, Z., ... & Yu, F. (2020). Citral-loaded chitosan/carboxymethyl cellulose copolymer hydrogel microspheres with improved antimicrobial effects for plant protection. *International Journal of Biological Macromolecules*, *164*, 986-993.

[29] Turek, C., & Stintzing, F. C. (2013). Stability of essential oils: a review. *Comprehensive reviews in food science and food safety*, 12(1), 40-53.

[30] Vasconcelos, N. G., Croda, J., & Simionatto, S. (2018). Antibacterial mechanisms of cinnamon and its constituents: A review. *Microbial pathogenesis,* 120, 198-203.

[31] Porfírio, E. M., Melo, H. M., Pereira, A. M. G., Cavalcante, T., Gomes, G. A., Carvalho, M., & Costa, R. (2017). In vitro antibacterial and antibiofilm activity of lippia alba essential oil, citral, and carvone against Staphylococcus aureus. *The Scientific World Journal,* 124(2), 379–388.

[32] Silva-Angulo, A. B., Zanini, S. F., Rodrigo, D., Klein, G., & Martine, A. (2015). Comparative study of the effects of citral on the growth and injury of Listeria innocua and Listeria monocytogenes cells. *Plos One,* 10(2).

[33] Belda-Galbis, C. M., Pina-Perez, M. C., Leufven, A., Martinez, A., & Rodrigo, D. (2013). Impact assessment of carvacrol and citral effect on Escherichia coli K12 and Listeria innocua growth. *Food Control*, 33(2), 536–544.

[34] Kang, S., Li, X., Xing, Z., Liu, X., Bai, X., Yang, Y., & Shi, C. (2022). Antibacterial effect of citral on yersinia enterocolitica and its mechanism. *Food Control,* 135, 108775.

[35] Tao, N., OuYang, Q., & Jia, L. (2014). Citral inhibits mycelial growth of Penicillium italicum by a membrane damage mechanism. Food Control, 41, 116-121.

[36] Trombetta, D., Castelli, F., Sarpietro, M. G., Venuti, V., Cristani, M., Daniele, C., ... & Bisignano, G. (2005). Mechanisms of antibacterial action of three monoterpenes. *Antimicrobial agents and chemotherapy,* 49(6), 2474-2478.

[37] Nimmagadda, A., Liu, X., Teng, P., Su, M., Li, Y., Qiao, Q., ... & Cai, J. (2017). Polycarbonates with potent and selective antimicrobial activity toward gram-positive bacteria. *Biomacromolecules*, *18*(1), 87-95.

[38] Tavares, T. D., Antunes, J. C., Padrão, J., Ribeiro, A. I., Zille, A., Amorim, M. T. P., ... & Felgueiras, H. P. (2020). Activity of specialized biomolecules against gram-positive and gram-negative bacteria. *Antibiotics*, *9*(6), 314.